



Published in final edited form as:

*Mol Cancer Res.* 2009 September ; 7(9): 1487–1496. doi:10.1158/1541-7786.MCR-09-0166.

## Bcl-2 Modulation to Activate Apoptosis in Prostate Cancer

Kevin Bray<sup>1,2</sup>, Hsin-Yi Chen<sup>1,2</sup>, Cristina M. Karp<sup>1</sup>, Michael May<sup>1</sup>, Shridar Ganesan<sup>1,3</sup>, Vassiliki Karantza-Wadsworth<sup>1,3</sup>, Robert S. DiPaola<sup>1,3</sup>, and Eileen White<sup>1,2</sup>

<sup>1</sup>The Cancer Institute of New Jersey, New Brunswick, New Jersey

<sup>2</sup>Rutgers University, Piscataway, New Jersey

<sup>3</sup>Division of Medical Oncology, Department of Internal Medicine, University of Medicine and Dentistry of New Jersey, Robert Wood Johnson Medical School

### Abstract

Apoptosis resistance is a hallmark of cancer linked to disease progression and treatment resistance, which has led to the development of anticancer therapeutics that restore apoptotic function. Antiapoptotic Bcl-2 is frequently overexpressed in refractory prostate cancer and increased following standard hormonal therapy and chemotherapy; however, the rationally designed Bcl-2 antagonist, ABT-737, has not shown single agent apoptosis-promoting activity against human prostate cancer cell lines. This is likely due to the coordinate expression of antiapoptotic, Bcl-2–related Mcl-1 that is not targeted by ABT-737. We developed a mouse model for prostate cancer in which apoptosis resistance and tumorigenesis were conferred by Bcl-2 expression. Combining ABT-737 with agents that target Mcl-1 sensitized prostate cancer cell lines with an apoptotic block to cell death *in vitro*. In mice *in vivo*, ABT-737 showed single agent efficacy in prostate tumor allografts in which tumor cells are under hypoxic stress. In human prostate cancer tissue, examined using a novel tumor explant system designated Tumor Tissue Assessment for Response to Chemotherapy, combination chemotherapy promoted efficient apoptosis. Thus, rational targeting of both the Bcl-2 and Mcl-1 mechanisms of apoptosis resistance may be therapeutically advantageous for advanced prostate cancer.

### Introduction

Advanced prostate cancer is only temporarily controlled by either androgen ablation therapy or chemotherapy due to mechanisms of drug resistance (1). Progression towards drug resistance can be achieved through the inactivation of apoptosis, and is generally considered to be a hallmark of cancer (2). Understanding these drug resistance mechanisms allows for the identification of ways to therapeutically reactivate the death response and a means to develop clinical trials to treat the disease (3,4).

Apoptosis is a highly controlled process activated in response to specific stimuli, cellular damage, stress, and chemotherapy leading to cellular dismantling within membrane-enclosed vesicles that are engulfed by phagocytes (5-7). Bcl-2 family members are key regulators in the apoptotic pathway (5,7). Bcl-2 family members fall into three classes based

Copyright © 2009 American Association for Cancer Research.

**Requests for reprints:** Eileen White, The Cancer Institute of New Jersey, 195 Little Albany Street, Room 2601, New Brunswick, NJ 08903-2681. Phone: 732-235-5329; Fax: 732-235-5795. whiteei@umdnj.edu.  
K Bray and H-Y. Chen contributed equally to this work.

**Disclosure of Potential Conflicts of Interest** Dr. Eileen White is a consultant for Merck, Millennium, BMS, and Chugai.

**Note:** Supplementary data for this article are available at Molecular Cancer Research Online (<http://mcr.aacrjournals.org/>).

on conserved homology domains (BH1-4): antiapoptotic multidomain (Bcl-2, Bcl-x<sub>L</sub>, Mcl-1, and Bfl-1/A1), proapoptotic multidomain (Bax and Bak), and BH3-only (Bid, Bad, Bim, Puma, and Noxa) proteins. Multidomain Bcl-2-like proteins contain a large hydrophobic cleft that is a receptor for the BH3  $\alpha$ -helix of essential apoptosis effectors Bax and Bak, which neutralizes their proapoptotic function (5,7,8). The BH3 of BH3-only proteins disrupts Bax and Bak sequestration and may also directly activate Bax and Bak. Once activated, Bax and Bak oligomerize in the mitochondrial outer membrane, releasing cytochrome *c*, which stimulates the apoptosome and promotes activation of the cysteine protease caspase-9 (6). Subsequent effector caspase-3 activation leads to the cleavage of cellular substrates and apoptotic cell death. Apoptosis is an effective cell-intrinsic tumor suppression mechanism to limit tumor initiation and progression, and is also a critical mechanism to facilitate tumor regression in cancer therapy.

Prostate cancer commonly exhibits high levels of Bcl-2 expression in refractory, advanced disease that contributes to defective apoptosis associated with poor prognosis (9). Modulating Bcl-2 in patients with prostate cancer is limited due to few therapeutic options (10-12). Mechanistic insight into apoptosis regulation has led to novel therapeutic approaches. For example, the hydrophobic cleft of antiapoptotic Bcl-2-like proteins has been targeted with small molecules as the basis for the BH3-mimetic class of Bcl-2-inhibitory, proapoptotic anticancer drugs (3). The Bcl-2 antagonist and BH3-mimetic ABT-737 binds with high affinity to the hydrophobic cleft and BH3 receptor region of Bcl-2, Bcl-x<sub>L</sub>, and Bcl-w, but not to the less homologous Bcl-2-related protein Mcl-1. This ABT-737/Bcl-2 interaction antagonizes the interaction of Bcl-2 with the BH3 domain of proapoptotic proteins, neutralizing Bcl-2. Although ABT-737 shows single agent activity promoting apoptosis in human small cell lung cancer and lymphoma cell lines *in vitro* and in tumor xenografts, apoptosis is not triggered in most human cancer cell lines (13-16). Expression of Mcl-1 that is not targeted by ABT-737 may explain the resistance of prostate and other cancer cell lines to apoptosis.

One means to inhibit Mcl-1, which is necessary but not sufficient for apoptosis, is activation of the DNA damage response pathway that targets Mcl-1 for proteasome-mediated degradation (17,18). Chemotherapeutic agents that directly induce DNA damage (etoposide and cisplatin) are expected to induce Mcl-1 elimination that occurs by a p53-independent mechanism (18,19). Furthermore, paclitaxel, which targets microtubules and induces Bim accumulation (antagonizing both Bcl-2 and Mcl-1; ref. 20), might promote apoptosis. Although taxanes and platinum agents have been used to treat prostate cancer, they are not effective against advanced disease, perhaps due to high levels of Bcl-2 which may inhibit apoptosis even when Mcl-1 is eliminated. Mcl-1 expression is known to increase during prostate cancer progression (21), indicating that it could be a potential clinical target. Thus, simultaneously targeting Bcl-2 and Mcl-1 could be a rational regimen in disease treatment.

Here, we report that paclitaxel, etoposide, and cisplatin act synergistically with the Bcl-2 antagonist ABT-737 to induce apoptosis in a mouse model for prostate cancer. The combination of ABT-737 with paclitaxel, etoposide, or cisplatin resulted in down-regulation of Mcl-1, cytochrome *c* release, and caspase-3 activation in immortalized mouse prostate epithelial cell lines that possess an apoptosis defect and are rendered tumorigenic through Bcl-2 expression. Surprisingly, ABT-737 promoted tumor regression as a single agent in immortalized mouse prostate tumor allografts, in which *in vivo* stress may provide signals to induce BH3-only proteins to antagonize Mcl-1. Importantly, cisplatin and ABT-737 act synergistically to induce apoptosis in a novel tumor explant system we have designated Tumor Tissue Assessment for Response to Chemotherapy (TTARC). Taken together, these preclinical data support the development of therapy with a platinum agent in combination with a Bcl-2 inhibitor in the treatment of prostate cancer.

## Results

### A Novel Mouse Model for Prostate Cancer

Most prostate cancers are adenocarcinomas arising from prostate epithelial cells (22). We developed a novel mouse model for prostate epithelial tumor progression and treatment responsiveness (23,24). Primary prostate epithelial cells were isolated from male C57B/6 mice and immortalized through the expression of E1A and a dominant-negative p53 to inactivate the Rb and p53 pathways (Fig. 1A). Eight independent immortal mouse prostate epithelial cell lines (iMPEC) were generated and characterized. Six iMPEC cell lines (2-7) formed fusion sheets, characteristic of epithelial cells in culture, whereas two (1 and 8) had fewer cell-cell junctions and a more mesenchymal morphology (Fig. 1A). All iMPECs express E1A and dominant-negative p53, as well as the androgen receptor, the prostate-specific homeobox protein Nkx3.1, and the epithelial cell marker  $\beta$ -catenin (Fig. 1B). Consistent with their morphologic appearance (Fig. 1A), iMPEC cell lines 2 to 7 expressed the luminal epithelial cell marker cytokeratin 8/18, whereas iMPEC cell lines 1 and 8 expressed the basal cell marker vimentin (Fig. 1B). This suggests that two prostate epithelial cell types, luminal and basal cells, were immortalized.

To evaluate apoptosis pathways, the endogenous expression of Bcl-2 family members was examined. All iMPECs express the antiapoptotic Bcl-2, Bcl-x<sub>L</sub>, Mcl-1, and proapoptotic Bax and Bak (Fig. 1C). iMPECs also express variable levels of Bim (Figs. 1C and 2B). iMPECs were poorly and clonally tumorigenic, indicating that inactivating the Rb and p53 pathways in mouse prostate epithelial cells was insufficient for tumorigenesis (Fig. 1D). Previously established work has shown that tumors which take longer than 2 months to appear require an additional genetic event to enable tumorigenesis (23-25). Mutations in *ras* genes (*H-ras*, *K-ras*, and *N-ras*) are associated with human prostate tumor progression (26-28), and H-Ras activation blocks apoptosis rendering iBMKs and iMMECs highly tumorigenic (20,29,30). As such, iMPEC-7 was engineered to express activated H-Ras<sup>V12</sup> (Supplementary Fig. S1), which conferred tumorigenicity (Fig. 1D).

### iMPECs Have an Intact p53-Independent Apoptotic Response

Because iMPECs express Bim (Figs. 1C and 2B), which is induced by and is a determinant of apoptotic response to taxanes (20,31), we examined iMPECs for apoptosis in response to paclitaxel. Paclitaxel (at 300 nmol/L and 1  $\mu$ mol/L) caused loss of viability (Fig. 2A) accompanied by robust Bim induction and caspase-3 activation (Fig. 2B), indicating an intact p53-independent apoptotic response in iMPECs. iMPECs show some variability; however, all responded to paclitaxel with Bim induction and apoptosis. As Bim is a potent Bcl-2 antagonist (32,33), and up-regulation of Bcl-2 is implicated in prostate cancer progression (34), this supports a prominent role of the Bim-Bcl-2 axis in the apoptotic response of prostate epithelial cells. This intact p53-independent apoptotic response may be responsible for defective tumorigenesis (Fig. 1D). To test this, iMPEC-7 was engineered to express human Bcl-2 (hBcl-2; Fig. 2C), which substantially blocks apoptosis (see below). Bcl-2 expression promoted tumorigenesis (Fig. 2D), although to a lesser extent than H-Ras<sup>V12</sup> (Fig. 1D). Bcl-2-expressing iMPEC tumors were carcinomas with well-vascularized sheets of epithelial cells and isolated areas of necrosis. Additionally, tumor tissue invaded the skeletal muscle (Fig. 2D, *inset*).

### ABT-737 Acts Synergistically with Paclitaxel to Induce Apoptosis

Because agents that target microtubules, such as the taxane docetaxel, have been clinically active against prostate cancer and can improve survival with temporary duration of response, we examined the apoptotic response of Bcl-2-expressing iMPECs to taxane chemotherapy. Bcl-2 expression conferred resistance to the taxane paclitaxel (Fig. 3). Accordingly, we

sought to determine if ABT-737 could act synergistically with paclitaxel to induce apoptosis. Paclitaxel (300 nmol/L) in combination with the less active enantiomer control for ABT-737 had no effect on cell viability in iMPECs with endogenous or hBcl-2 expression (Fig. 3A), whereas 1  $\mu$ mol/L of paclitaxel alone or with the enantiomer resulted in the cell death of iMPECs with endogenous Bcl-2 expression. In contrast, 0.1  $\mu$ mol/L of ABT-737 in combination with 300 nmol/L of paclitaxel was sufficient to kill 70% of iMPECs with endogenous Bcl-2 in 3 days (Fig. 3A, *top*). hBcl-2-expressing iMPECs required 10  $\mu$ mol/L of ABT-737 with 300 nmol/L of paclitaxel to induce similar levels of apoptosis induction (Fig. 3A, *bottom*). The ABT-737/paclitaxel combination induced cytochrome *c* release and high levels of caspase-3 activation (Fig. 3B-D; Supplementary Fig. S2). iMPECs with endogenous Bcl-2 had higher levels of cytochrome *c* release and activated caspase-3 when compared with hBcl-2-expressing iMPECs. Combination of paclitaxel with the enantiomer resulted in some cytochrome *c* release and caspase-3 activation, but overall levels were significantly higher with the ABT-737/paclitaxel combination (Fig. 3B-D; Supplementary Fig. S2). This showed that a taxane could act synergistically with ABT-737 to induce apoptosis in prostate cancer cell lines, thereby overcoming an apoptosis block conferred by hBcl-2.

### ABT-737 Restores Apoptosis in Combination with DNA-Damaging Agents

We next tested whether ABT-737 in combination with DNA-damaging agents that target the antiapoptotic Mcl-1 protein could overcome an apoptotic block conferred by hBcl-2. The viability of iMPECs was assessed with ABT-737, or the enantiomer, with or without cisplatin, an alkylating agent that forms DNA adducts or etoposide, a topoisomerase II inhibitor that induces DNA breaks. The combination of 12.5  $\mu$ mol/L of cisplatin and 0.1  $\mu$ mol/L of ABT-737 effectively killed 90% of iMPECs with endogenous Bcl-2 (Fig. 4A, *top*). Cisplatin (12.5  $\mu$ mol/L) induced a 50% reduction in viability within 3 days in iMPECs with endogenous Bcl-2, but was unable to kill hBcl-2-expressing iMPECs, whereas a combination of 25  $\mu$ mol/L of cisplatin and 10  $\mu$ mol/L of ABT-737 was required to kill 90% of iMPECs expressing hBcl-2 (Fig. 4A). This showed that hBcl-2 expression produced resistance to cisplatin-mediated apoptosis, and that ABT-737 was not an effective inducer of cell death as a single agent. As expected, cisplatin treatment down-regulated the levels of Mcl-1 over 3 days in both iMPECs with endogenous Bcl-2 and those with hBcl-2 (Fig. 4C). ABT-737/cisplatin combination resulted in cytochrome *c* release and activation of caspase-3, even with hBcl-2 expression (Fig. 4B-D; Supplementary Fig. S3). This showed that ABT-737, when used in combination with DNA-damaging agents, effectively induced apoptosis in cells normally refractory to cell death. Interestingly, Bcl-2 levels were down-regulated in response to higher concentrations of ABT-737 and cisplatin (Fig. 4C). Similar results were achieved when etoposide was used in combination with ABT-737, suggesting a general synergy between DNA damage and Bcl-2 antagonism (Supplementary Fig. S4).

### ABT-737 Promotes the Regression of Prostate Tumor Allografts

Because ABT-737 and cisplatin displayed synergy *in vitro* and could overcome apoptosis resistance conferred by Bcl-2, we investigated the response of mouse prostate tumor allografts to combination therapy. iMPECs expressing hBcl-2 were injected s.c. into mice and allowed to form tumors. ABT-737 was injected i.p. at a dose of 100 mg/kg/d for 14 consecutive days. Cisplatin was injected i.p. at a dose of 2.5 mg/kg on days 1 and 8. Vehicle and cisplatin injections had no effect on tumor growth, whereas ABT-737 and the ABT-737/cisplatin combination prevented tumor growth and promoted tumor regression (Fig. 5A and B). Thus, the response to Bcl-2 inhibition can be different *in vivo* compared with *in vitro*.

## ABT-737 and Cisplatin Promote Apoptosis in Human Prostate Tumor Tissue Explants

The conflicting requirement of cisplatin for synergy with a Bcl-2 antagonist for apoptosis activation *in vitro* versus *in vivo* raised the question as to what to expect for therapeutic apoptosis modulation in human prostate cancer therapy. To assess the potential effectiveness of chemotherapy in patients with prostate cancer, in which access to tumor tissue during treatment is limited, we developed a novel tumor explant system designated TTARC wherein tumor tissue is assessed for apoptotic response to therapy *ex vivo*. Briefly, human prostatectomy samples were obtained immediately following surgery, and sectioned to generate successive adjacent tumor tissue slices from the same tumor (Fig. 6A). Tissue sections were left untreated or treated with ABT-737, the enantiomer, cisplatin, or the combination of cisplatin and ABT-737 or the enantiomer. Five human prostate tumors were analyzed by TTARC, and remarkably, tissue remained healthy for at least 16 hours, as indicated by H&E staining of healthy epithelial cells in the glands with intact stroma (Fig. 6B) that was similar to sections fixed at the start of the incubation (time 0). Treatment duration varied from 16 to 48 hours and was compared with time 0. Two different concentrations of ABT-737 were tested (1 and 10  $\mu\text{mol/L}$ ). Although there was some variability in the integrity of the samples and in the levels of apoptosis induced, it was clear that the combination of ABT-737 and cisplatin was the most effective apoptosis inducer. The control enantiomer of ABT-737 induced minimal levels of apoptosis alone or in combination with cisplatin (Fig. 6; data not shown). Incubation with either 12.5  $\mu\text{mol/L}$  of cisplatin or 10  $\mu\text{mol/L}$  of ABT-737 resulted in little or no induction of apoptosis (Fig. 6B; Table 1). In contrast, the same concentrations of ABT-737 in combination with cisplatin induced significantly higher levels of activated caspase-3 and obvious signs of epithelial tissue degradation, i.e., elimination of tumor cells from the tissue (Fig. 6B; Table 1). Assessing active caspase-3 at specific times of treatment provides a snapshot of apoptosis activity and the enhanced tissue degradation in combination drug-treated tissues likely reflects accelerated apoptosis and possible necrotic cell death. This indicated that combination of a Bcl-2 antagonist with cisplatin could overcome apoptosis resistance in human prostate tumor tissue and provides preclinical justification for therapeutic treatment development.

## Discussion

As in many cancers, defective signaling of apoptosis likely contributes to treatment failure, and in advanced prostate cancer, is associated with high levels of Bcl-2 (9). However, in most cancers, it seems unlikely that targeting Bcl-2 alone will be sufficient for apoptosis induction due to functionally redundant Bcl-2 family members, particularly Mcl-1 (35-38). Similarly, targeting only Mcl-1 is also insufficient for apoptosis induction in cancer cell lines (17,18,38). Strategies to activate apoptosis through modulation of Bcl-2 family members may require neutralization of multiple antiapoptotic Bcl-2-related proteins (8,38).

Proper targeting will depend on knowing which Bcl-2-related proteins are expressed and are essential for blocking apoptosis in particular cancers. The BH3-mimetic ABT-737 (15) and the orally available relative ABT-263 (39) neutralize multiple Bcl-2-related proteins (Bcl-2, Bcl-x<sub>L</sub>, and Bcl-w) but not Mcl-1 (14,37,39). ABT-737 as a single agent is insufficient to induce apoptosis in most cancer cell lines and xenografts (15,37) as well as in normal tissues with the exception of platelets, which are particularly reliant on Bcl-x<sub>L</sub> for survival (40,41). As such, a BH3 mimetic that neutralizes Mcl-1, for example, would be a valuable strategy to obtain synergy with ABT-737 for apoptosis induction. Alternatively, inhibition of Mcl-1 by indirect means such as DNA damage should achieve similar results. Indeed, synergy between ABT-737 and a platinum agent has been reported to promote apoptosis in ovarian cancer cell lines *in vitro* (42), as we have reported here in prostate cancer cell lines. Upstream of Bcl-2 and Mcl-1, the proapoptotic BH3-only protein Bim is an epithelial tumor

suppressor that is dramatically up-regulated in response to taxane-based chemotherapy (20). We observed similar Bim induction associated with caspase-3 activation and apoptosis by paclitaxel in iMPECs. By virtue of its broad binding specificity, Bim may be critically important for modulating apoptosis. Indeed, Bim is a tumor suppressor in Myc-induced lymphomas and promotes apoptosis in conjunction with imatinib in human leukemia cell lines (43). However, high levels of Bcl-2 expression are sufficient to block apoptosis and render iMPECs and other cell lines tumorigenic, and taxane-mediated Bim induction is insufficient to overcome this apoptotic block conferred by Bcl-2. Moreover, antagonizing Bcl-2 with ABT-737 was insufficient to trigger apoptosis. In contrast, combining ABT-737 with a taxane or DNA-damaging agent caused a dramatic induction of apoptosis in prostate cancer cell lines *in vitro*, suggesting the possible utility of these combinations for prostate cancer therapy (Fig. 6C).

Surprisingly, ABT-737 displayed single-agent efficacy in mouse prostate tumor allografts. Thus, the apoptotic response can vary greatly between *in vitro* and *in vivo* situations. In contrast to growth *in vitro*, tumors *in vivo* are subjected to hypoxia and the induction of BH3-only proteins such as Puma and activation of Bim-mediated Bax and Bak-dependent apoptosis and tumor repression (20). Because Puma and Bim are proapoptotic BH3-only proteins with broad-spectrum-binding activity toward antiapoptotic Bcl-2 family members including Mcl-1, the *in vivo* environment may provide signals to induce Mcl-1 antagonists, explaining why ABT-737 displayed single-agent efficacy. Alternatively, subcutaneously grown mouse prostate tumors are very distinct from spontaneous human prostate cancers with respect to stroma and microenvironment. Subcutaneous tumors have markedly less stroma and when subjected to TTARC, undergo accelerated disintegration when compared with human prostate cancer tissue. These dramatic differences between apoptotic responses of tumor cells *in vitro* and *in vivo* raised questions about the predictability of patient responses.

Although mouse models are tremendously valuable for functional validation of mechanisms involved in cancer modulation, in many cases, they fail to accurately represent the diversity and complexity found in human cancers. It may be that the substantial stromal components and natural microenvironment in the prostate helps to maintain tissue integrity (including tumor tissue) which influences responses to chemotherapy and supports survival. This is yet another mechanism by which tumors grown subcutaneously in a mouse may respond differently from tumors spontaneously arising in tissues. Effective drug treatments in xenograft models often have little efficacy in the clinic. The outcome of such experiments is dependent on many variables, such as site of implantation, growth properties of xenografts, tumor size when treatment is initiated, agent formulation, route of administration and dose, and selected end point for assessing activity (44-46). In contrast, mechanistic assessment and validation of cancer treatment in solid tumor-bearing humans can be problematic due to limited or insufficient access to tumor tissue, disease diversity, and lack of molecular characterization of individual tumors. In human prostate cancer, the limited access to tumor tissue during treatment precludes determination that a particular treatment is effective by the expected mechanism. Assessment of surrogate markers as indicators of mechanistic validation is a common alternative but is not ideal as it is often not clear if normal tissues reflect the properties of tumors often derived from completely different tissue types. The means to bridge the gap between mouse cancer models and human cancers, both with their inherent strengths and weaknesses, has been a major issue in the field of cancer research.

To bridge this gap, we have developed an *ex vivo* tumor tissue explant system (TTARC). The concept was to take cancer-containing prostatectomy samples that retain tumor tissue and stroma intact in thin tissue slices that can be incubated in cell culture media for short periods of time during which the apoptotic response (active caspase-3) to chemotherapy

could be assessed. Remarkably, the tissue remained healthy as assessed by histologic appearance. Tumor tissue disruption and isolation of tumor cells typically results in a poor rate of cell survival, but retaining the tumor cells, associated stroma, and microenvironment intact in tissue slices apparently provided a substantial survival advantage. Similar results have been obtained using the TTARC system with human breast and ovarian cancer samples (data not shown). Multiple tissue slices were obtained from each prostatectomy sample which enabled the analysis of replicates and allowed for time course doseresponse and drug combination assessment that would have otherwise been difficult or impossible to assess in human cancers by available means.

When evaluated for apoptosis induction by cisplatin, ABT-737 alone or in combination, the combination produced a striking activation of caspase-3 and cell death. These findings were reproducible in multiple prostatectomy samples and the tumor cells within the tissue seemed to be more susceptible to apoptosis activation compared with the neighboring normal prostate epithelia. The different response of tumor allografts (and potentially xenografts) to ABT-737 suggests that apoptotic therapeutic response is highly context-dependent. Spontaneous tumors that coevolve with stroma and tissue microenvironment may be under less stress compared with transplanted tumor cells and this may be reflected in altered response to chemotherapy. This suggests that improving the assessment of the response to chemotherapy of human tumors may be advantageous. The development of TTARC enables preclinical assessment of chemotherapeutics in human cancer prior to the treatment of patients. This will become increasingly valuable as a preclinical justification for new clinical trials. In future studies, it will be important to correlate the results of TTARC with response to chemotherapy and clinical outcome. As such, combining cisplatin and perhaps paclitaxel with the BH3-mimetic ABT-737 may be a worthwhile approach to prostate cancer therapy.

## Materials and Methods

### Generation of Cell Lines

Prostates from 6-wk-old male C57Bl/6 mice were used to generate immortalized mouse prostate epithelial cells as previously described (23,24,47). Stable cell lines expressing H-Ras<sup>V12</sup>, hBcl-2, or vector control were derived through electroporation of pcDNA3.1-hBcl-2 (48), pCGN-H-Ras<sup>V12</sup>, or pcDNA3.1 (Invitrogen) followed by geneticin (Life Technologies-Invitrogen) selection.

### Chemicals and 3-(4,5-Dimethylthiazol-2-yl)2,5-Diphenyltetrazolium Bromide Assay

3-(4,5-Dimethylthiazol-2-yl)2,5-diphenyltetrazolium bromide (MTT assay) and cisplatin were from Sigma, etoposide and paclitaxel were from Calbiochem, and ABT-737 and control enantiomer were from Abbott Laboratories. ABT-737 and its enantiomer were prepared in DMSO and stored at  $-20^{\circ}\text{C}$ .

### Western Blotting, Immunofluorescence, and Immunohistochemistry

Western blotting and immunofluorescence was done as previously described (17,49,50). For cytochrome *c* detection, cells were fixed in 4% paraformaldehyde (Sigma), and for caspase-3 immunofluorescence, cells were fixed with Formalde-fresh (Fisher Scientific) for 15 min at room temperature.

The following antibodies were used: E1A (M73), p53 (Ab-1), and actin (Ab-1; Oncogene); androgen receptor, Nkx 3.1 (generously provided by Dr. Cory Abate-Shen, Department of Urology, Columbia University, New York, NY);  $\beta$ -catenin (Zymed); cytokeratin 8/18, HA. 11 (Covance); vimentin (generously provided by Dr. Robert Evans, Department of Pathology, University of Colorado, Denver, CO); Bcl-2 (sc-7382; Santa Cruz

Biotechnology); Bax/Bak (Upstate Biotechnology); Bim (Axxora); Mcl-1 (Rockland); cleaved caspase-3 (Asp175; Cell Signaling); and Bcl-x<sub>L</sub> and cytochrome *c* (PharMingen).

### Tumor Formation and Chemotherapy

Tumor formation and volume in nude mice was done as previously described (24). Tumor formation assays were done using Institutional Animal Care and Use–approved protocols. Tumors for histology were fixed with Formalde-fresh (Fisher Scientific). For chemotherapeutic experiments, when iMPEC-7\_Bcl-2 tumors reached 80 to 90 mm<sup>3</sup>, mice were assorted randomly into groups of six and subjected to i.p. injection of vehicle, cisplatin (2.5 mg/kg on days 1 and 8), ABT-737 (100 mg/kg/d for 14 d), or cisplatin in combination with ABT-737. For i.p. injection, ABT-737 was prepared in 30% propylene glycol, 5% Tween 20, and 65% D5W (5% dextrose in water). Cisplatin was prepared in PBS.

### The TTARC System

Human prostatectomy samples were obtained from the Tissue Analytical Services at The Cancer Institute of New Jersey immediately following surgery. Vibratome-sliced samples (200 μm) were placed on gel foam/surgifoam (Ethicon) in DMEM plus 10% fetal bovine serum with or without drugs. Sections were fixed in Formalde-fresh (Fisher Scientific) for 1 h and transferred to 70% ethanol. Immunohistochemistry and histology were done as described (50). Prostate tissue sections were scored based on intensity of staining. *P* values were determined by assigning the number of “+” signs a numeral value, i.e., “++++” would be assigned a value of 4. These numbers were then used to calculate *P* values via one-way ANOVA with Bonferroni’s post-test (GraphPad Prism 4). Institutional Review Board approval was obtained for these experiments.

### Supplementary Material

Refer to Web version on PubMed Central for supplementary material.

### Acknowledgments

We thank Thomasina Sharkey for assistance with manuscript preparation; Drs. Cory Abate-Shen and Robert Evans for providing antibodies; Drs. Steven Elmore, Saul Rosenberg, and Steven Fesik at Abbott Laboratories for supplying ABT-737 and the enantiomer; the Tissue Analytical Services at The Cancer Institute of New Jersey for providing the human prostatectomy samples and tissue sectioning; and the members of the White lab for helpful advice.

**Grant support:** NIH grants R37CA53370 and RO1CA130893 (E. White), DOD grants W81XWH05-I-0235 and 06314001 (R.S. DiPaola and E. White). K. Bray was supported by Training Grant (2T32 AI007403).

### References

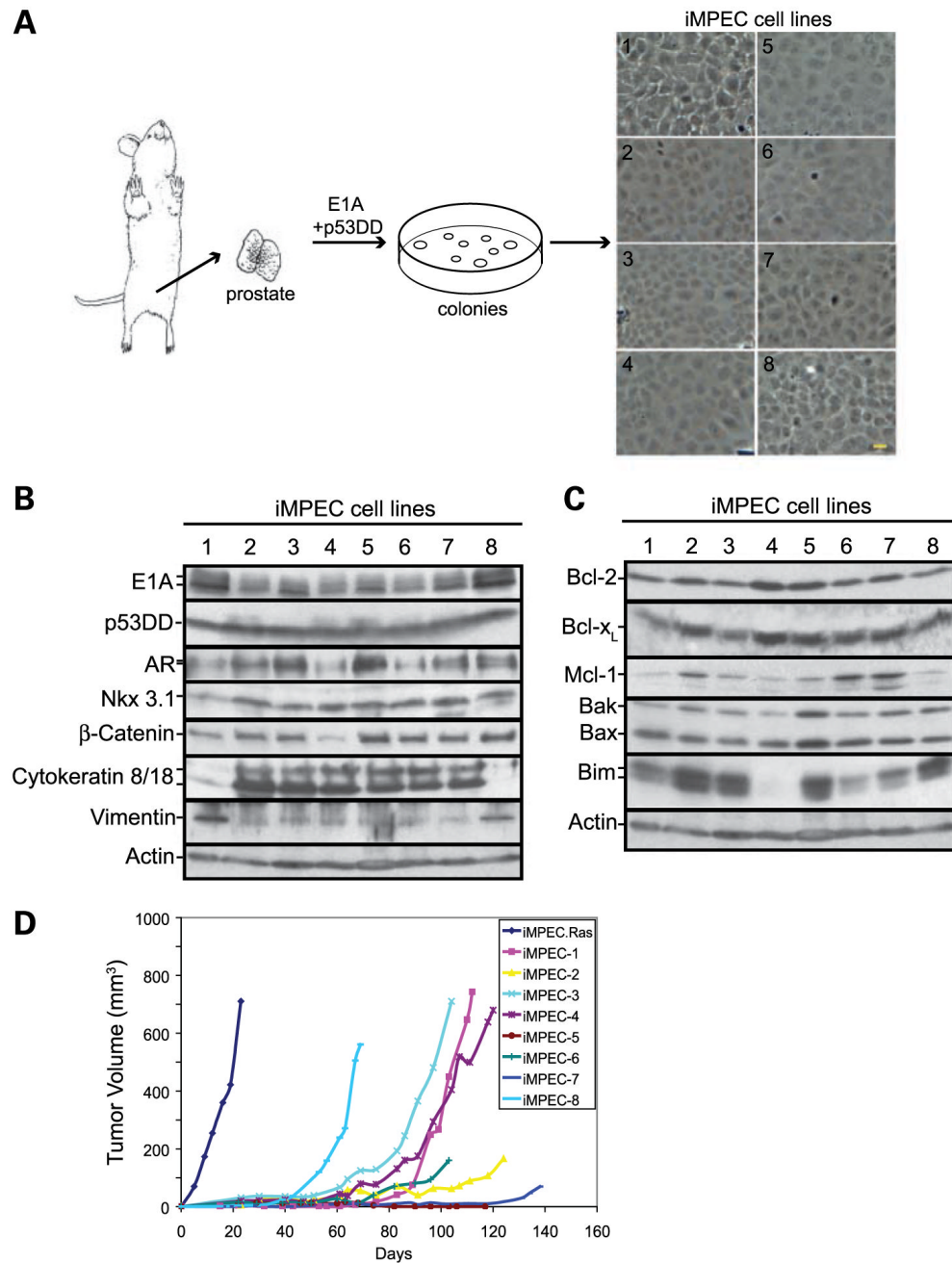
1. Petrylak DP. Chemotherapy for androgen-independent prostate cancer. *World J Urol* 2005;23:10–3. [PubMed: 15685445]
2. Hanahan D, Weinberg RA. The hallmarks of cancer. *Cell* 2000;100:57–70. [PubMed: 10647931]
3. Fesik SW. Promoting apoptosis as a strategy for cancer drug discovery. *Nat Rev Cancer* 2005;5:876–85. [PubMed: 16239906]
4. Karantza-Wadsworth, V.; White, E. Programmed cell death. In: DeVita, VT.; Lawrence, TS.; Rosenberg, SA., editors. *Cancer: principles and practice of oncology*. 8th ed. Lippincott, Williams, & Wilkins; Baltimore: 2008. p. 93-101.
5. Adams JM, Cory S. Bcl-2-regulated apoptosis: mechanism and therapeutic potential. *Curr Opin Immunol* 2007;19:488–96. [PubMed: 17629468]
6. Green DR, Kroemer G. The pathophysiology of mitochondrial cell death. *Science* 2004;305:626–9. [PubMed: 15286356]



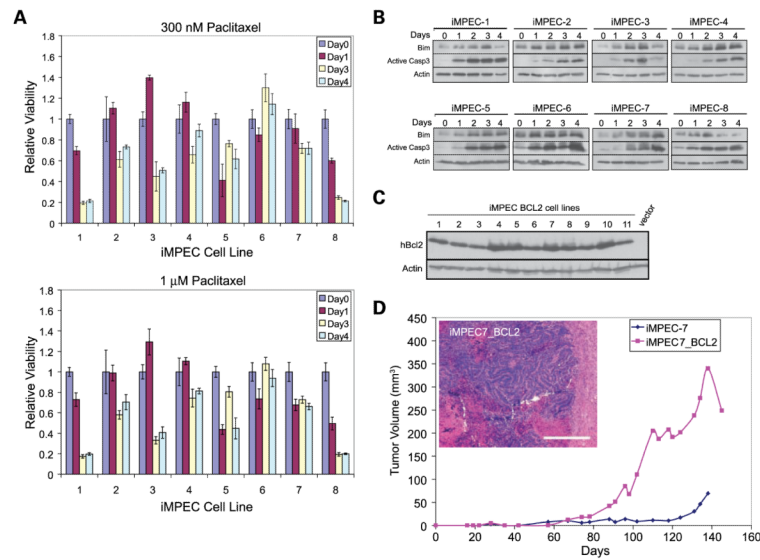
7. Danial NN, Korsmeyer SJ. Cell death: critical control points. *Cell* 2004;116:205–19. [PubMed: 14744432]
8. Gelinas C, White E. BH3-only proteins in control: specificity regulates MCL-1 and BAK-mediated apoptosis. *Genes Dev* 2005;19:1263–8. [PubMed: 15937216]
9. McDonnell TJ, Troncoso P, Brisbay SM, et al. Expression of the protooncogene bcl-2 in the prostate and its association with emergence of androgen-independent prostate cancer. *Cancer Res* 1992;52:6940–4. [PubMed: 1458483]
10. DiPaola RS, Rafi MM, Vyas V, et al. Phase I clinical and pharmacologic study of 13-*cis*-retinoic acid, interferon alfa, and paclitaxel in patients with prostate cancer and other advanced malignancies. *J Clin Oncol* 1999;17:2213–8. [PubMed: 10561278]
11. Morris MJ, Cordon-Cardo C, Kelly WK, et al. Safety and biologic activity of intravenous BCL-2 antisense oligonucleotide (G3139) and taxane chemotherapy in patients with advanced cancer. *Appl Immunohistochem Mol Morphol* 2005;13:6–13. [PubMed: 15722787]
12. Morris MJ, Tong WP, Cordon-Cardo C, et al. Phase I trial of BCL-2 anti-sense oligonucleotide (G3139) administered by continuous intravenous infusion in patients with advanced cancer. *Clin Cancer Res* 2002;8:679–83. [PubMed: 11895895]
13. Deng J, Carlson N, Takeyama K, Cin P Dal, Shipp M, Letai A. BH3 profiling identifies three distinct classes of apoptotic blocks to predict response to ABT-737 and conventional chemotherapeutic agents. *Cancer Cell* 2007;12:171–85. [PubMed: 17692808]
14. Konopleva M, Contractor R, Tsao T, et al. Mechanisms of apoptosis sensitivity and resistance to the BH3 mimetic ABT-737 in acute myeloid leukemia. *Cancer Cell* 2006;10:375–88. [PubMed: 17097560]
15. Oltersdorf T, Elmore SW, Shoemaker AR, et al. An inhibitor of Bcl-2 family proteins induces regression of solid tumours. *Nature* 2005;435:677–81. [PubMed: 15902208]
16. Tahir SK, Yang X, Anderson MG, et al. Influence of Bcl-2 family members on the cellular response of small-cell lung cancer cell lines to ABT-737. *Cancer Res* 2007;67:1176–83. [PubMed: 17283153]
17. Cuconati A, Mukherjee C, Perez D, White E. DNA damage response and MCL-1 destruction initiate apoptosis in adenovirus-infected cells. *Genes Dev* 2003;17:2922–32. [PubMed: 14633975]
18. Nijhawan D, Fang M, Traer E, et al. Elimination of Mcl-1 is required for the initiation of apoptosis following ultraviolet irradiation. *Genes Dev* 2003;17:1475–86. [PubMed: 12783855]
19. Yang C, Kaushal V, Shah SV, Kaushal GP. Mcl-1 is downregulated in cis-platin-induced apoptosis, and proteasome inhibitors restore Mcl-1 and promote survival in renal tubular epithelial cells. *Am J Physiol Renal Physiol* 2007;292:F1710–7. [PubMed: 17311906]
20. Tan TT, Degenhardt K, Nelson DA, et al. Key roles of BIM-driven apoptosis in epithelial tumors and rational chemotherapy. *Cancer Cell* 2005;7:227–38. [PubMed: 15766661]
21. Krajewska M, Krajewski S, Epstein JI, et al. Immunohistochemical analysis of bcl-2, bax, bcl-X, and mcl-1 expression in prostate cancers. *Am J Pathol* 1996;148:1567–76. [PubMed: 8623925]
22. Bostwick DG. The pathology of early prostate cancer. *CA Cancer J Clin* 1989;39:376–93. [PubMed: 2482118]
23. Degenhardt K, White E. A mouse model system to genetically dissect the molecular mechanisms regulating tumorigenesis. *Clin Cancer Res* 2006;12:5298–304. [PubMed: 17000662]
24. Mathew R, Degenhardt K, Haramaty L, Karp CM, White E. Chapter 5 immortalized mouse epithelial cell models to study the role of apoptosis in cancer. *Methods Enzymol* 2008;446:77–106. [PubMed: 18603117]
25. Karp CM, Tan TT, Mathew R, et al. Role of the polarity determinant crumbs in suppressing mammalian epithelial tumor progression. *Cancer Res* 2008;68:4105–15. [PubMed: 18519669]
26. Anwar K, Nakakuki K, Shiraishi T, Naiki H, Yatani R, Inuzuka M. Presence of ras oncogene mutations and human papillomavirus DNA in human prostate carcinomas. *Cancer Res* 1992;52:5991–6. [PubMed: 1382850]
27. Carter BS, Epstein JI, Isaacs WB. ras gene mutations in human prostate cancer. *Cancer Res* 1990;50:6830–2. [PubMed: 2208148]
28. Watanabe M, Shiraishi T, Yatani R, Nomura AM, Stemmermann GN. International comparison on ras gene mutations in latent prostate carcinoma. *Int J Cancer* 1994;58:174–8. [PubMed: 8026877]

29. Rijnders AW, van der Korput JA, van Steenbrugge GJ, Romijn JC, Trapman J. Expression of cellular oncogenes in human prostatic carcinoma cell lines. *Biochem Biophys Res Commun* 1985;132:548–54. [PubMed: 3904752]
30. Karantza-Wadsworth V, Patel S, Kravchuk O, et al. Autophagy mitigates metabolic stress and genome damage in mammary tumorigenesis. *Genes Dev* 2007;21:1621–35. [PubMed: 17606641]
31. Bouillet P, Metcalf D, Huang DC, et al. Proapoptotic Bcl-2 relative Bim required for certain apoptotic responses, leukocyte homeostasis, and to preclude autoimmunity. *Science* 1999;286:1735–8. [PubMed: 10576740]
32. Certo M, Del Gaizo Moore V, Nishino M, et al. Mitochondria primed by death signals determine cellular addiction to antiapoptotic BCL-2 family members. *Cancer Cell* 2006;9:351–65. [PubMed: 16697956]
33. Bouillet P, Cory S, Zhang LC, Strasser A, Adams JM. Degenerative disorders caused by Bcl-2 deficiency prevented by loss of its BH3-only antagonist Bim. *Dev Cell* 2001;1:645–53. [PubMed: 11709185]
34. Bruckheimer EM, Brisbay S, Johnson DJ, Gingrich JR, Greenberg N, McDonnell TJ. Bcl-2 accelerates multistep prostate carcinogenesis *in vivo*. *Oncogene* 2000;19:5251–8. [PubMed: 11077442]
35. Chen L, Willis SN, Wei A, et al. Differential targeting of prosurvival Bcl-2 proteins by their BH3-only ligands allows complementary apoptotic function. *Mol Cell* 2005;17:393–403. [PubMed: 15694340]
36. Chen S, Dai Y, Harada H, Dent P, Grant S. Mcl-1 down-regulation potentiates ABT-737 lethality by cooperatively inducing Bak activation and Bax translocation. *Cancer Res* 2007;67:782–91. [PubMed: 17234790]
37. van Delft MF, Wei AH, Mason KD, et al. The BH3 mimetic ABT-737 targets selective Bcl-2 proteins and efficiently induces apoptosis via Bak/Bax if Mcl-1 is neutralized. *Cancer Cell* 2006;10:389–99. [PubMed: 17097561]
38. Willis SN, Chen L, Dewson G, et al. Proapoptotic Bak is sequestered by Mcl-1 and Bcl-xL, but not Bcl-2, until displaced by BH3-only proteins. *Genes Dev* 2005;19:1294–305. [PubMed: 15901672]
39. Tse C, Shoemaker AR, Adickes J, et al. ABT-263: a potent and orally bio-available Bcl-2 family inhibitor. *Cancer Res* 2008;68:3421–8. [PubMed: 18451170]
40. Mason KD, Carpinelli MR, Fletcher JI, et al. Programmed anuclear cell death delimits platelet life span. *Cell* 2007;128:1173–86. [PubMed: 17382885]
41. Zhang H, Nimmer PM, Tahir SK, et al. Bcl-2 family proteins are essential for platelet survival. *Cell Death Differ* 2007;14:943–51. [PubMed: 17205078]
42. Witham J, Valenti MR, De-Haven-Brandon AK, et al. The Bcl-2/Bcl-XL family inhibitor ABT-737 sensitizes ovarian cancer cells to carboplatin. *Clin Cancer Res* 2007;13:7191–8. [PubMed: 18056200]
43. Kuroda J, Puthalakath H, Cragg MS, et al. Bim and Bad mediate imatinib-induced killing of Bcr/Abl+ leukemic cells, and resistance due to their loss is overcome by a BH3 mimetic. *Proc Natl Acad Sci U S A* 2006;103:14907–12. [PubMed: 16997913]
44. Kelland LR. Of mice and men: values and liabilities of the athymic nude mouse model in anticancer drug development. *Eur J Cancer* 2004;40:827–36. [PubMed: 15120038]
45. Kerbel RS. Human tumor xenografts as predictive preclinical models for anticancer drug activity in humans: better than commonly perceived—but they can be improved. *Cancer Biol Ther* 2003;2:S134–9. [PubMed: 14508091]
46. Takimoto CH. Why drugs fail: of mice and men revisited. *Clin Cancer Res* 2001;7:229–30. [PubMed: 11234873]
47. Degenhardt K, Chen G, Lindsten T, White E. BAX and BAK mediate p53-independent suppression of tumorigenesis. *Cancer Cell* 2002;2:193–203. [PubMed: 12242152]
48. Kasof GM, Goyal L, White E. Btf, a novel death-promoting transcriptional repressor that interacts with Bcl-2-related proteins. *Mol Cell Biol* 1999;19:4390–404. [PubMed: 10330179]
49. Degenhardt K, Sundararajan R, Lindsten T, Thompson C, White E. Bax and Bak independently promote cytochrome C release from mitochondria. *J Biol Chem* 2002;277:14127–34. [PubMed: 11836241]

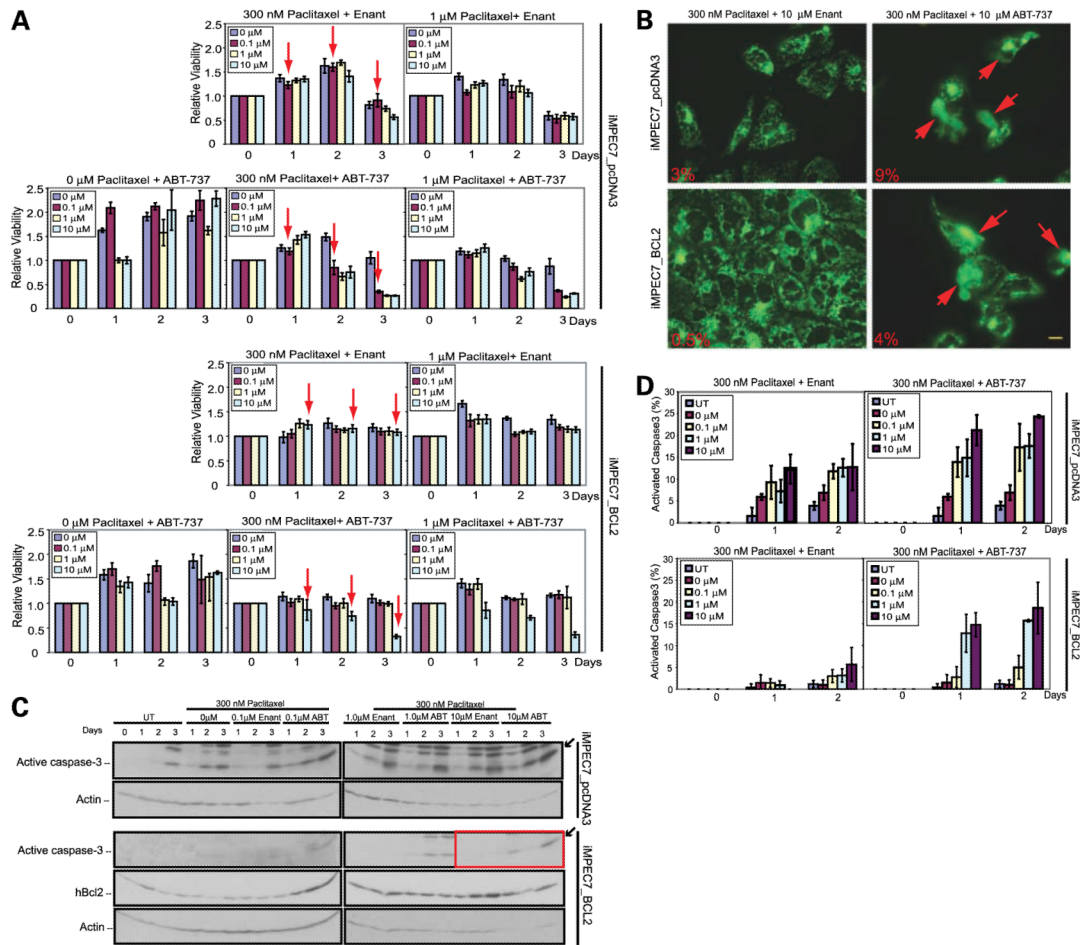
50. Nelson DA, Tan TT, Rabson AB, Anderson D, Degenhardt K, White E. Hypoxia and defective apoptosis drive genomic instability and tumorigenesis. *Genes Dev* 2004;18:2095–107. [PubMed: 15314031]



**FIGURE 1.** Generation of iMPEC cell lines. **A.**Immortalization of primary mouse prostate epithelial cell lines. Prostate cells were isolated and immortalized by transfection of E1A and dominant-negative p53. Bar, 10  $\mu$ m. **B.** Western blot analysis of E1A, p53DD, AR, Nkx3.1,  $\beta$ -catenin, cytokeratin 8/18, and vimentin of iMPEC cell lines 1 to 8. **C.** Western blot of endogenous expression of proapoptotic and antiapoptotic proteins. **D.** Tumor formation of iMPECs and an iMPEC\_H-Ras<sup>V12</sup>. iMPECs are poorly tumorigenic.

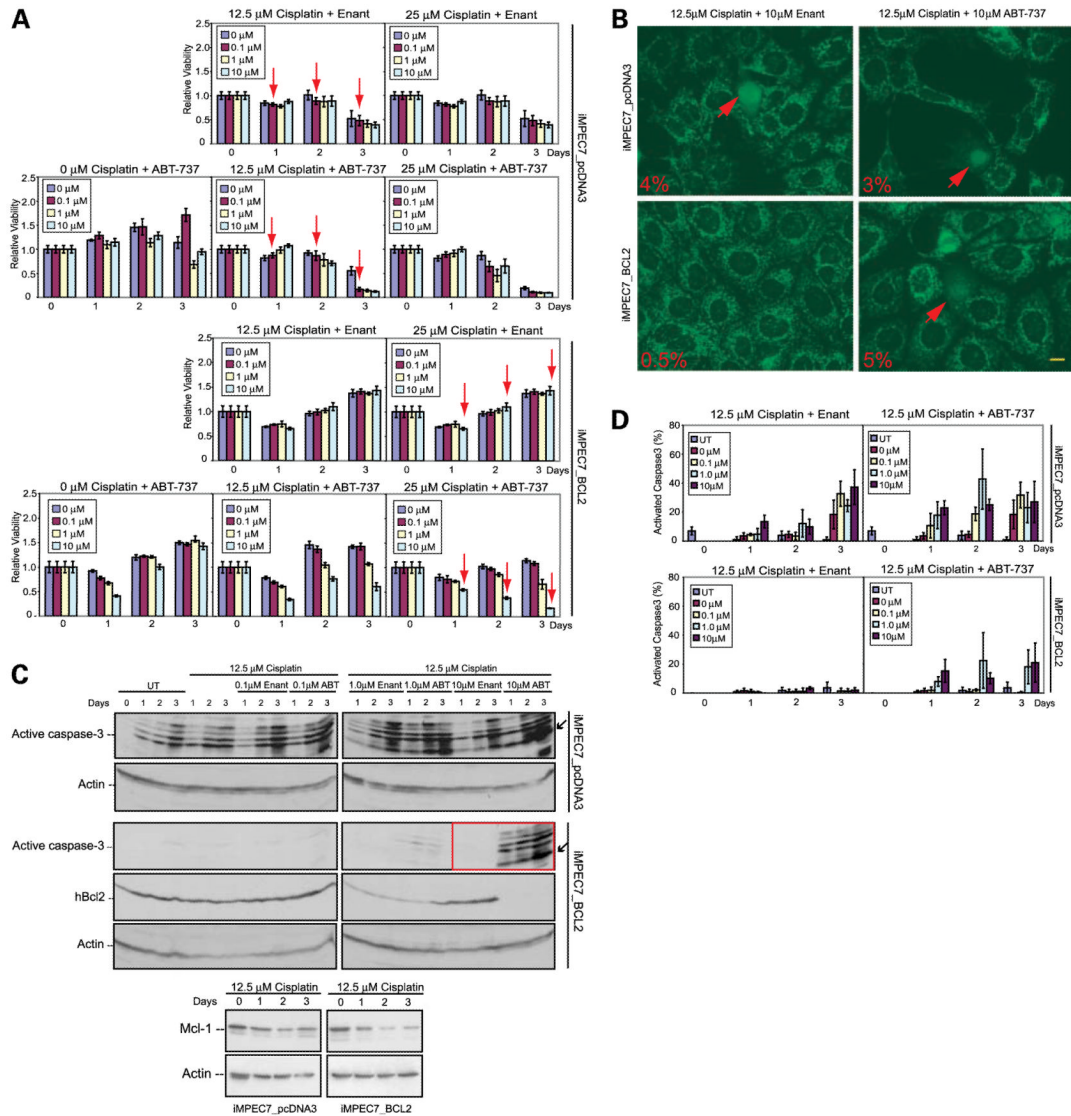


**FIGURE 2.** iMPECs respond to paclitaxel with Bim induction and caspase-3 activation indicative of an intact p53-independent apoptotic response. **A.** MTT assay of iMPEC cell lines (1-8) in response to 300 nmol/L or 1 μmol/L of paclitaxel after 1 to 4 d. Viabilities are relative to time 0. **B.** Western blots showing iMPEC cell lines treated with 300 nmol/L of paclitaxel for 1 to 4 d respond by induction of Bim and activation of caspase-3. **C.** Western blots of hBcl-2 expression in iMPECs engineered to express human Bcl-2. **D.** Tumor formation of iMPEC-7 and a derived cell line (no. 4) expressing hBcl-2. Bcl-2 expression promotes tumorigenesis. Inset, H&E staining of a tumor from an iMPEC\_Bcl-2 cell line. Bar, 50 μm.



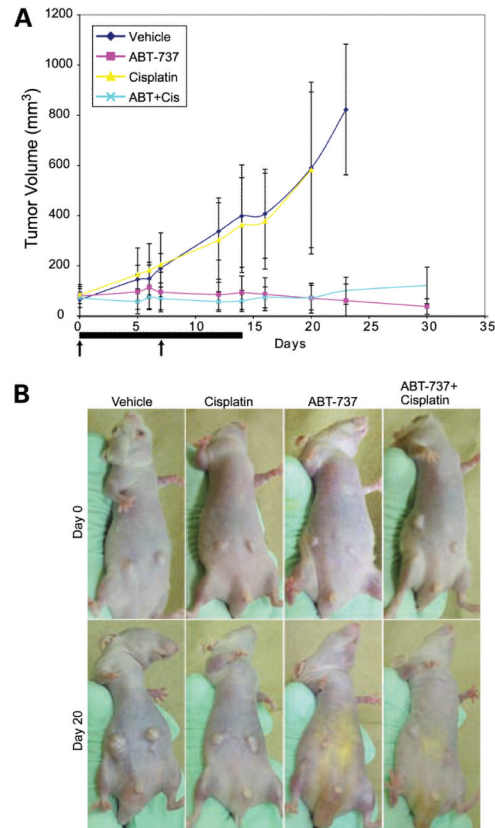
**FIGURE 3.**

ABT-737 acts synergistically with paclitaxel to induce apoptosis. **A.** MTT assay of iMPEC-7\_pcDNA3 (*top*) and iMPEC-7\_Bcl-2 (*bottom*). iMPEC-7\_pcDNA3 was killed with lower concentrations of ABT-737/paclitaxel than iMPEC-7\_Bcl-2 (*arrows*). Viabilities are relative to time 0. **B.** Indirect immunofluorescence for cytochrome *c* release. iMPEC-7\_pcDNA3 and iMPEC-7\_Bcl-2 were treated with 300 nmol/L of paclitaxel and 10 μmol/L of ABT-737 for 2 d. Arrows, cells with released cytochrome *c*. Percentage of cytochrome *c* release (*bottom left corner of each image*). Bar, 10 μm. **C.** iMPEC-7\_Bcl-2 showed caspase-3 activation in response to 10 μmol/L of ABT-737 and 300 nmol/L of paclitaxel (*box*). **D.** Quantitation of activated caspase-3. ABT-737/paclitaxel combination induced high levels of active caspase-3 at 2 d. Bars, SD based on three independent experiments.



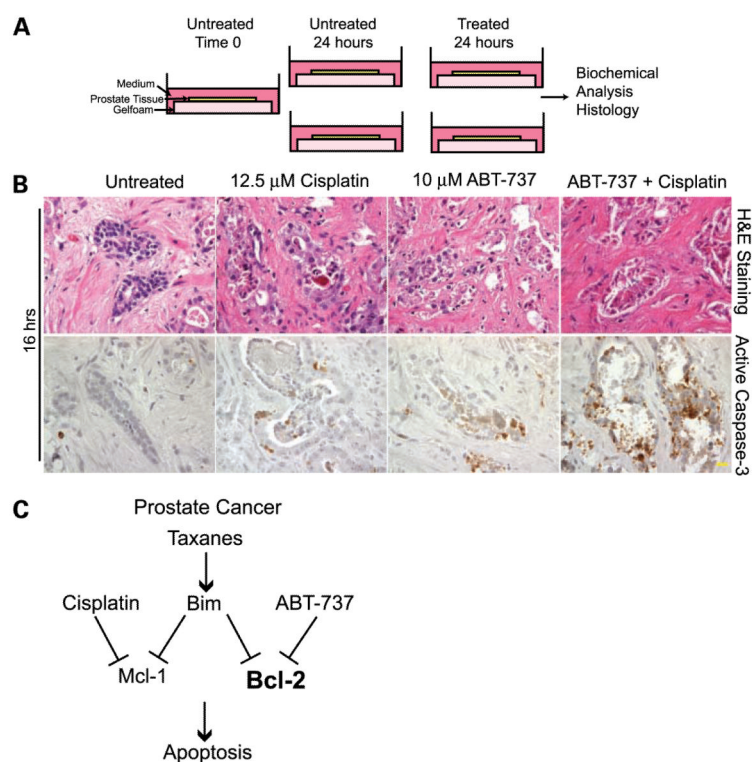
**FIGURE 4.**

ABT-737 in combination with cisplatin induces apoptosis. **A**, MTT assay of iMPEC-7\_pcDNA3 (top) and iMPEC-7\_Bcl-2 (bottom). iMPEC-7\_pcDNA3 and iMPEC-7\_Bcl-2 showed sensitivity to the ABT-737/cisplatin combination. iMPEC-7\_pcDNA3 was killed with lower concentrations of ABT-737/cisplatin than iMPEC-7\_Bcl-2 (arrows). Viabilities are relative to time 0. **B**, Indirect immunofluorescence for cytochrome *c* release. Arrows, cells with released cytochrome *c* at 3 d. Percentage of cytochrome *c* release (bottom left corner of each image). Bar, 10 μm. **C**, iMPEC-7\_Bcl-2 showed high levels of active caspase-3 in response to 10 μmol/L of ABT-737 and 12.5 μm of cisplatin (top, red box). Western blot showing Mcl-1 levels with 12.5 μmol/L of cisplatin in iMPEC\_pcDNA3 and iMPEC\_Bcl-2 cells (bottom). **D**, Quantitation of activated caspase-3. Bars, SD based on three independent experiments.

**FIGURE 5.**

ABT-737 inhibits tumor growth in mouse allografts. **A.** iMPEC-7\_Bcl-2 cells were inoculated subcutaneously into nude mice to form tumors. Bar, the 14-d ABT-737 dosing period. Arrows, days that cisplatin was dosed. ABT-737 (*purple line*) and ABT-737/cisplatin (*light blue line*) inhibited tumor growth when compared with vehicle (*dark blue line*) or cisplatin alone (*yellow line*). Bars, SDs from six mice in each experimental group. **B.** Images of subcutaneous tumors on representative mice from each group.



**FIGURE 6.**

*Ex vivo* chemotherapeutic response of human prostate tumor tissue explants. **A.** TTARC. Human prostatectomy samples were sectioned to generate 200 μm slices and placed onto gelfoam in wells with medium. **B.** Human prostate tumor tissue sections (tumor 3) were treated with cisplatin and ABT-737 as single agents or in combination for 16 h and subjected to H&E staining or immunohistochemistry for activated caspase-3. Untreated tissue remained viable under normal tissue culture conditions (*H&E, left*). Combination of cisplatin and ABT-737 resulted in the destruction of epithelial tissue components (**H&E, right**), and high levels of caspase-3 activation (*right*), indicating that tissue degradation was the result of apoptosis induced by the ABT-737/cisplatin combination. Magnification, ×600. Bar, 10 μm. **C.** Model for overcoming apoptotic resistance in prostate cancer.

**Table 1**

## Five Human Prostate Tumors Examined Using TTARC

Tumor	Drug concentration	Treatment duration (h)	Active caspase-3
Tumor 1	Untreated	24	++
	10 $\mu\text{mol/L}$ Enantiomer	24	++
	12.5 $\mu\text{mol/L}$ Cisplatin	24	++
	10 $\mu\text{mol/L}$ ABT-737	24	+
	Ctl + Cis	24	++
	ABT + Cis	24	++++
Tumor 2	Untreated	24	-
	10 $\mu\text{mol/L}$ Enantiomer	24	-
	12.5 $\mu\text{mol/L}$ Cisplatin	24	+
	10 $\mu\text{mol/L}$ ABT-737	24	+
	Ctl + Cis	24	+
	ABT + Cis	24	++
Tumor 3	Untreated	16	-
	10 $\mu\text{mol/L}$ Enantiomer	16	+
	12.5 $\mu\text{mol/L}$ Cisplatin	16	++
	10 $\mu\text{mol/L}$ ABT-737	16	++
	Ctl + Cis	16	++
	ABT + Cis	16	++++
Tumor 4	Untreated	48	+
	10 $\mu\text{mol/L}$ Enantiomer	48	+
	12.5 $\mu\text{mol/L}$ Cisplatin	48	++
	10 $\mu\text{mol/L}$ ABT-737	48	++
	Ctl + Cis	48	+
	ABT + Cis	48	++++
Tumor 5	Untreated	24	++
	1 $\mu\text{mol/L}$ Enantiomer	24	+
	12.5 $\mu\text{mol/L}$ Cisplatin	24	+++
	1 $\mu\text{mol/L}$ ABT-737	24	++
	Ctl + Cis	24	++
	ABT + Cis	24	++++

NOTES: The ABT-737/cisplatin combination was a significantly stronger inducer of apoptosis when compared with untreated ( $P < 0.001$ ), the control enantiomer ( $P < 0.001$ ), cisplatin alone ( $P < 0.01$ ), ABT-737 alone ( $P < 0.001$ ), or a combination of the control enantiomer and cisplatin ( $P < 0.001$ ). (-) no active caspase-3 staining; (+) positive active caspase-3 staining, in which the number of "+" symbols indicates the level of positive staining.